

An Absolute Sodium Cation Affinity Scale: Threshold Collision-Induced Dissociation Experiments and *ab Initio* Theory

P. B. Armentrout*

Department of Chemistry, University of Utah, Salt Lake City, Utah 84112

M. T. Rodgers

Department of Chemistry, Wayne State University, Detroit, Michigan 48202

Received: May 25, 1999; In Final Form: July 29, 1999

Threshold collision-induced dissociation of $\text{Na}^+(\text{L})$ with xenon is studied using guided ion beam mass spectrometry. The ligand L includes ethene, benzene, phenol, ammonia, acetaldehyde, acetone, and *N,N*-dimethylformamide. In all cases, the primary product formed corresponds to endothermic loss of the neutral ligand and the only other product observed is the result of ligand exchange processes to form NaXe^+ . The cross-section thresholds are interpreted to yield 0 and 298 K bond energies for Na^+-L after accounting for the effects of multiple ion–molecule collisions, internal energy of the reactant ions, and dissociation lifetimes. *Ab initio* calculations at several levels of theory compare favorably to the experimentally determined bond energies for these and previously studied systems, $\text{L} = \text{Ar}, \text{CO}, \text{dimethyl ether}, \text{H}_2\text{O}, \text{methylamine}, \text{imidazole}, \text{dimethoxyethane},$ and several alcohols. Combined, these ligands cover a very wide range in binding energies, and thereby help to establish an absolute scale for sodium cation affinities.

Introduction

In a recent article, Hoyau et al.¹ comprehensively reviewed experimental and theoretical values for the binding of sodium cations to small molecules. They noted that use of sodium cationized adducts of biologically relevant molecules had become extensive in mass spectrometric studies in recent years. The need to establish a reliable absolute sodium cation affinity scale to understand these studies was therefore apparent. To this end, they performed new experimental studies using pulsed ionization high-pressure mass spectrometry (PHPMS) of the complexes of Na^+ with methanol, ammonia, methylamine, and acetone. Their bond dissociation energy (BDE) for $\text{Na}^+(\text{NH}_3)$ was over 12 kJ/mol below two values from the literature, one from equilibrium HPMS studies of Castleman and co-workers² and the other from early threshold collision-induced dissociation measurements of Marinelli and Squires.³ Likewise, their BDE for $\text{Na}^+(\text{CH}_3\text{COCH}_3)$ lay 10 kJ/mol below values from Castleman and co-workers⁴ and a value determined by Feng and Gronert⁵ using the kinetic method and anchored to values determined by CID studies of Kebarle and co-workers.⁶ Their $\text{Na}^+(\text{CH}_3\text{NH}_2)$ and $\text{Na}^+(\text{CH}_3\text{OH})$ BDEs lay 24 and 11 kJ/mol, respectively, below values determined by Castleman and co-workers.⁴ Recent threshold CID work in our laboratory on the sodium cation affinities of the alcohols,⁷ however, obtained an even lower bond energy for $\text{Na}^+(\text{CH}_3\text{OH})$, supporting the experimental results of Hoyau et al. In this work, we also obtained a bond energy for $\text{Na}^+(2\text{-C}_3\text{H}_7\text{OH})$ that was lower than the results of Feng and Gronert⁵ by 10 kJ/mol. Further, our CID measurements of the bonding between Na^+ and the simple ligand CO ⁸ and a complex bidentate ligand, dimethoxyethane $[(\text{CH}_3\text{OCH}_2)_2]$,⁹ yield much lower values (by 19 and 38 kJ/mol, respectively) than work of Castleman and co-workers.¹⁰

In addition to these experimental studies, Hoyau et al. calculated the sodium cation affinities of 28 molecules including

many for which experimental data were available, as well as several systems for which no experiments had been performed. Agreement between their own experiments and theory was excellent, within 4 kJ/mol, and within experimental error of values from our group concerning water¹¹ and imidazole.¹² Their calculated value for $\text{Na}^+(\text{H}_2\text{O})$ is somewhat below (by about 8 kJ/mol) that measured by Dzidic and Kebarle¹³ using HPMS and by Burdett and Hayhurst¹⁴ using flame mass spectrometry. The theoretical values generally disagreed with the experimental and theoretical results from Feng and Gronert⁵ and with the equilibrium HPMS studies of Castleman and co-workers for the molecules noted above and for several additional systems, including benzene,¹⁵ for which no other experimental results are available.

Because there appeared to be several controversial values in the compilation of Hoyau et al.,¹ we decided to augment the experimental database by directly measuring the absolute bond dissociation energies (BDEs) of $\text{Na}^+(\text{L})$ species using threshold CID in a guided ion beam mass spectrometer. The present study includes the following ligands: $\text{L} = \text{ethene}, \text{benzene}, \text{phenol}, \text{ammonia}, \text{acetaldehyde}, \text{acetone},$ and *N,N*-dimethylformamide. Ammonia and acetone were chosen to provide overlap with the experimental studies of Hoyau et al. Ethene, benzene, and phenol were chosen as examples of systems where the metal cation binds through the π -electrons on the ligand, interactions of significant importance in understanding biological systems. As noted above, previous experimental studies of the benzene, ammonia, acetone, and *N,N*-dimethylformamide complexes have been conducted. This work constitutes the first experimental determinations of the BDEs of the sodiated complexes of ethene, phenol, and acetaldehyde.

Theoretical calculations at the MP2(full)/6-31G* levels are carried out to provide structures, vibrational frequencies, and rotational constants needed for the analysis of the threshold CID data. The present experimental BDEs are compared to binding

* Corresponding author.

energies calculated at several levels of theory, including the MP2 level of theory recommended by Hoyau et al.¹ and density functional methods. To help verify the accuracy of these calculations, we also perform calculations using several compound methods designed to obtain energies with high accuracy, specifically, G2¹⁶ and G3¹⁷ theories, and the complete basis set extrapolation protocols, CBS-4, CBS-4M, and CBS-Q.^{18,19} We also perform these calculations for additional mono-ligated sodium cation complexes previously studied in our laboratory, a total of 18 molecules. Combined, these complexes span a broad range of binding energies, such that these comparisons help to provide a firm foundation for an absolute sodium cation affinity scale.

Experimental and Computational Section

General Experimental Procedures. Cross sections for CID of sodium cationized ligands are measured using a guided ion beam mass spectrometer that has been described in detail previously.^{20,21} The metal–ligand complexes are generated as described below. The ions are extracted from the source, accelerated, and focused into a magnetic sector momentum analyzer for mass analysis. Mass-selected ions are decelerated to a desired kinetic energy and focused into an octopole ion guide, which traps the ions in the radial direction.²² The octopole passes through a static gas cell containing xenon, used as the collision gas, for reasons described elsewhere.^{23–25} Low gas pressures in the cell (typically 0.05 to 0.20 mTorr) are used to ensure that multiple ion–molecule collisions are improbable. Product and unreacted beam ions drift to the end of the octopole where they are focused into a quadrupole mass filter for mass analysis and subsequently detected with a secondary electron scintillation detector and standard pulse counting techniques. Ion intensities are converted to absolute cross sections as described previously.²⁰ Absolute uncertainties in cross section magnitudes are estimated to be $\pm 20\%$, and are largely the result of uncertainties in the pressure measurement and the length of the interaction region.

Ion kinetic energies in the laboratory frame, E_{lab} , are converted to energies in the center of mass frame, E_{CM} , using the formula $E_{\text{CM}} = E_{\text{lab}} m/(m+M)$, where M and m are the masses of the ionic and neutral reactants, respectively. All energies reported below are in the CM frame unless otherwise noted. The absolute zero and distribution of the ion kinetic energies are determined using the octopole ion guide as a retarding potential analyzer as previously described.²⁸ Because the reaction zone and energy analysis region are physically the same, ambiguities in the energy analysis resulting from contact potentials, space charge effects, and focusing aberrations are minimized.²⁰ The distribution of ion kinetic energies is nearly Gaussian with a fwhm typically between 0.2 and 0.3 eV (lab) for these experiments. The uncertainty in the absolute energy scale is ± 0.05 eV (lab).

Even when the pressure of the reactant neutral is low, we have previously demonstrated that the effects of multiple collisions can significantly influence the shape of CID cross sections.²⁶ Because the presence and magnitude of these pressure effects is difficult to predict, we have performed pressure-dependent studies of all cross sections examined here. In the present systems, we observe small cross sections at low energies that have an obvious dependence upon pressure. We attribute this to multiple energizing collisions that lead to an enhanced probability of dissociation below threshold as a result of the longer residence time of these slower-moving ions. Data free from pressure effects are obtained by extrapolating to zero reactant pressure, as described previously.²⁶ Thus, results reported below are due to single bimolecular encounters.

Ion Source. The sodium cation complexes are formed in a 1 m long flow tube^{21,27} operating at a pressure of 0.5–0.7 Torr with a helium flow rate of about 6000 sccm. Sodium ions are generated in a continuous dc discharge by argon ion sputtering of a cathode, made from tantalum, with a cavity containing sodium metal. Typical operating conditions of the discharge are about 1.4–1.8 kV and 20–30 mA in a flow of roughly 10% argon in helium. The $\text{Na}^+(\text{L})$ complexes are formed by associative reactions of the sodium ion with a neutral ligand that is introduced into the flow 50 cm downstream from the dc discharge. The flow conditions used in this ion source provide in excess of 10^4 collisions between an ion and the buffer gas, which should thermalize the ions both vibrationally and rotationally. In our analysis of the data, we assume that the ions produced in this source are in their ground electronic states and that the internal energy of the $\text{Na}^+(\text{L})$ complexes is well described by a Maxwell–Boltzmann distribution of ro-vibrational states at 300 K. Previous work from this laboratory has shown that these assumptions are generally valid.^{26–31}

Thermochemical Analysis. The threshold regions of the reaction cross sections are modeled using eq 1,

$$\sigma(E) = \sigma_0 \sum_i g_i (E + E_i - E_0)^n / E \quad (1)$$

where σ_0 is an energy-independent scaling factor, E is the relative translational energy of the reactants, E_0 is the threshold for reaction of the ground electronic and ro-vibrational state, and n is an adjustable parameter. The summation is over the ro-vibrational states of the reactant ions, i , where E_i is the excitation energy of each state and g_i is the population of those states ($\sum g_i = 1$). The populations of excited ro-vibrational levels are not negligible even at 300 K as a result of the many low-frequency modes present in these ions. The relative reactivities of all ro-vibrational states, as reflected by σ_0 and n , are assumed to be equivalent. Vibrational frequencies and rotational constants are taken from ab initio calculations as detailed in the next section. The Beyer–Swinehart algorithm³² is used to evaluate the density of the ro-vibrational states, and the relative populations g_i are calculated by an appropriate Maxwell–Boltzmann distribution at the 300 K temperature appropriate for the reactants. We have estimated the sensitivity of our analysis to the deviations from the true frequencies by scaling the calculated frequencies to encompass the range of average valence coordinate scale factors needed to bring calculated frequencies into agreement with experimentally determined frequencies found by Pople et al.³³ Thus, the originally calculated vibrational frequencies were increased and decreased by 10%. The corresponding changes in the data analysis are included in the uncertainties listed with the E_0 values and other fitting parameters.

We also consider the possibility that collisionally activated complex ions do not dissociate on the time scale of our experiment (about 10^{-4} s) by including statistical theories for unimolecular dissociation into eq 1 as described in detail elsewhere.^{29,34,35} The details of the treatment for this lifetime effect that are used here parallel those for $\text{Na}^+(\text{alcohol})$ complexes recently published.⁷

The model represented by eq 1 is expected to be appropriate for translationally driven reactions³⁶ and has been found to reproduce reaction cross sections well in a number of previous studies of both atom–diatom and polyatomic reactions,^{25,37} including CID processes.^{26–29,34,35,38,39} The model is convoluted with the kinetic energy distributions of both reactants, and a nonlinear least-squares analysis of the data is performed to give

optimized values for the parameters σ_0 , E_0 , and n . The error associated with the measurement of E_0 is estimated from the range of threshold values determined for different data sets, variations associated with uncertainties in the vibrational frequencies, and the error in the absolute energy scale, 0.05 eV (lab). For analyses that include the lifetime effect, uncertainties in the reported E_0 values also include the effects of increasing and decreasing the time assumed available for dissociation (10^{-4} s) by a factor of 2.

Equation 1 explicitly includes the internal energy of the ion, E_i . All energy available is treated statistically, which should be a reasonable assumption because the internal (rotational and vibrational) energy of the reactants is redistributed throughout the ion upon impact with the collision gas. The threshold for dissociation is by definition the minimum energy required for dissociation and thus corresponds to formation of products with no internal excitation. The assumption that products formed at threshold have an internal temperature of 0 K has been tested for several systems.^{26–29,34,35,39} It has been shown that treating all energy of the ion (vibrational, rotational, and translational) as capable of coupling into the dissociation coordinate leads to reasonable thermochemistry. The threshold energies for dissociation reactions determined by analysis with eq 1 are converted to 0 K bond energies by assuming that E_0 represents the energy difference between reactants and products at 0 K.⁴⁰ This requires that there are no activation barriers in excess of the endothermicity of dissociation. This is generally true for ion–molecule reactions²⁵ and should be valid for the simple heterolytic bond fission reactions examined here.⁴¹

Computational Details. To obtain model structures, vibrational frequencies, and energetics for the neutral and sodiated ligands, ab initio calculations were carried out using Gaussian 98.⁴² These calculations include complexes for L = Ar, CO, ethene, benzene, methanol, dimethyl ether, water, phenol, ethanol, ammonia, 1-propanol, 2-propanol, acetaldehyde, acetone, imidazole, *N,N*-dimethylformamide, and dimethoxyethane [(CH₃OCH₂)₂], all studied experimentally in our laboratory, and methylamine, previously studied by Hoyau et al.¹ Geometry optimizations were performed at the MP2(full)/6-31G* level. This level of theory was recently determined by Hoyau et al. to be adequate for a good description of sodium cation complexes.¹ This conclusion is reinvestigated here. Vibrational analyses of the geometry-optimized structures were performed to determine the vibrational frequencies and rotational constants of the molecules. Such constants are listed for the seven systems studied experimentally in Tables S1 and S2, available in the supplementary information. When used to model the data or to calculate thermal energy corrections, the MP2(full)/6-31G* vibrational frequencies are scaled by a factor of 0.9646.^{15,43}

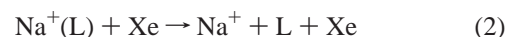
Single-point energy calculations were performed at the MP2-(full)/6-311+G(2d,2p) level using the MP2(full)/6-31G* geometries. To obtain accurate bond dissociation energies, basis set superposition errors (BSSE) were subtracted from the computed dissociation energies in the full counterpoise approximation^{44,45} as in several other recent papers on Na⁺ complexes.^{1,46,47} The BSSE corrections ranged from 2.1 kJ/mol for Na⁺(Ar) to 10.1 kJ/mol for the Na⁺[(CH₃OCH₂)₂] complexes. We also performed calculations using density functional theory using the B3LYP and B3P86 hybrid functionals, which utilize Becke's three-parameter functional⁴⁸ and the correlation functionals of Lee, Yang, and Parr (LYP)⁴⁹ or of Perdew (P86).⁵⁰ In both cases, geometry optimizations were performed using the 6-31G* basis set followed by single-point calculations (including BSSE corrections) using the 6-311+G(2d,2p) basis

set. Zero-point energy calculations use the scaled frequencies calculated at the MP2(full)/6-31G* level. Here BSSE corrections for the B3P86 calculations ranged from 0.7 kJ/mol for Na⁺(Ar) to 3.4 kJ/mol for Na⁺[(CH₃OCH₂)₂] and slightly smaller values for the B3LYP calculations.

To test the accuracy of these theoretical predictions, we also carried out complete basis set extrapolations at the CBS-4, CBS-4M, and CBS-Q levels of theory^{18,19} for all complexes. The CBS-4 model theory includes corrections for higher-order correlation effects calculated at the MP4 level with a modest-sized basis set (6-31G), but may be limited by the geometry optimization which is conducted at the HF/3-21G* level. The CBS-4M model is a revised version of the CBS-4 model that includes improved empirical parameters and a more stable minimal population localization procedure. The CBS-Q calculations determine geometries at the MP2(FC)/6-31G⁺ level and include higher-order correlation corrections at the MP4 and QCISD(T) levels of theory. For most of the complexes (excluding phenol and dimethoxyethane), we also carried out G2 calculations¹⁶ which determine geometries at the MP2(full)/6-31G* level and again include higher-order correlation corrections at the MP4 and QCISD(T) levels of theory. For the smallest complexes (all those with ligands containing less than four heavy atoms and that with acetone), we also performed G3 calculations which introduce additional improved correction terms and varies the higher-order correlation calculations. All these calculations were carried out using the Gaussian 98⁴² suite of programs.

Results

Cross Sections for Collision-Induced Dissociation. Experimental cross sections were obtained for the interaction of Xe with Na⁺(C₂H₄), Na⁺(C₆H₆), Na⁺(C₆H₅OH), Na⁺(ND₃), Na⁺(CH₃CHO), Na⁺[(CH₃)₂CO], and Na⁺[(CH₃)₂NCHO], complexes. Figure 1 shows data for all seven systems. The most favorable process observed for all complexes is the loss of the intact ligand in the collision-induced dissociation (CID) reactions 2.



The only other product observed in these reactions is the result of ligand exchange processes to form NaXe⁺. In all cases, thresholds for NaXe⁺ are slightly lower than for Na⁺ (by the Na⁺–Xe binding energy), although this is only apparent when the thresholds for the NaXe⁺ cross sections (not generally visible on the logarithmic scales of Figure 1) are examined. For the more strongly bound and complex ligands, the NaXe⁺ cross sections are small and rise slowly so that the apparent thresholds observed in Figure 1 are considerably higher than the energies where these cross sections first rise above zero. As little systematic information can be gleaned from these products, they will not be discussed further. However, it is conceivable that this ligand exchange process might cause a competitive shift in the observed thresholds. Within the quoted experimental errors, we do not believe such competition is likely to affect our threshold measurements in any of these systems for several reasons that have been detailed elsewhere.⁵¹

Threshold Analysis. The model of eq 1 was used to analyze the thresholds for reactions 2 in all seven Na⁺(L) systems. The results of these analyses are provided in Table 1 and shown in Figure 2. The experimental cross sections for reaction 2 in all seven systems are accurately reproduced over energy ranges exceeding 2 eV (3 eV for benzene, 4 eV for acetone and *N,N*-dimethylformamide, and 5 eV for the phenol and acetaldehyde

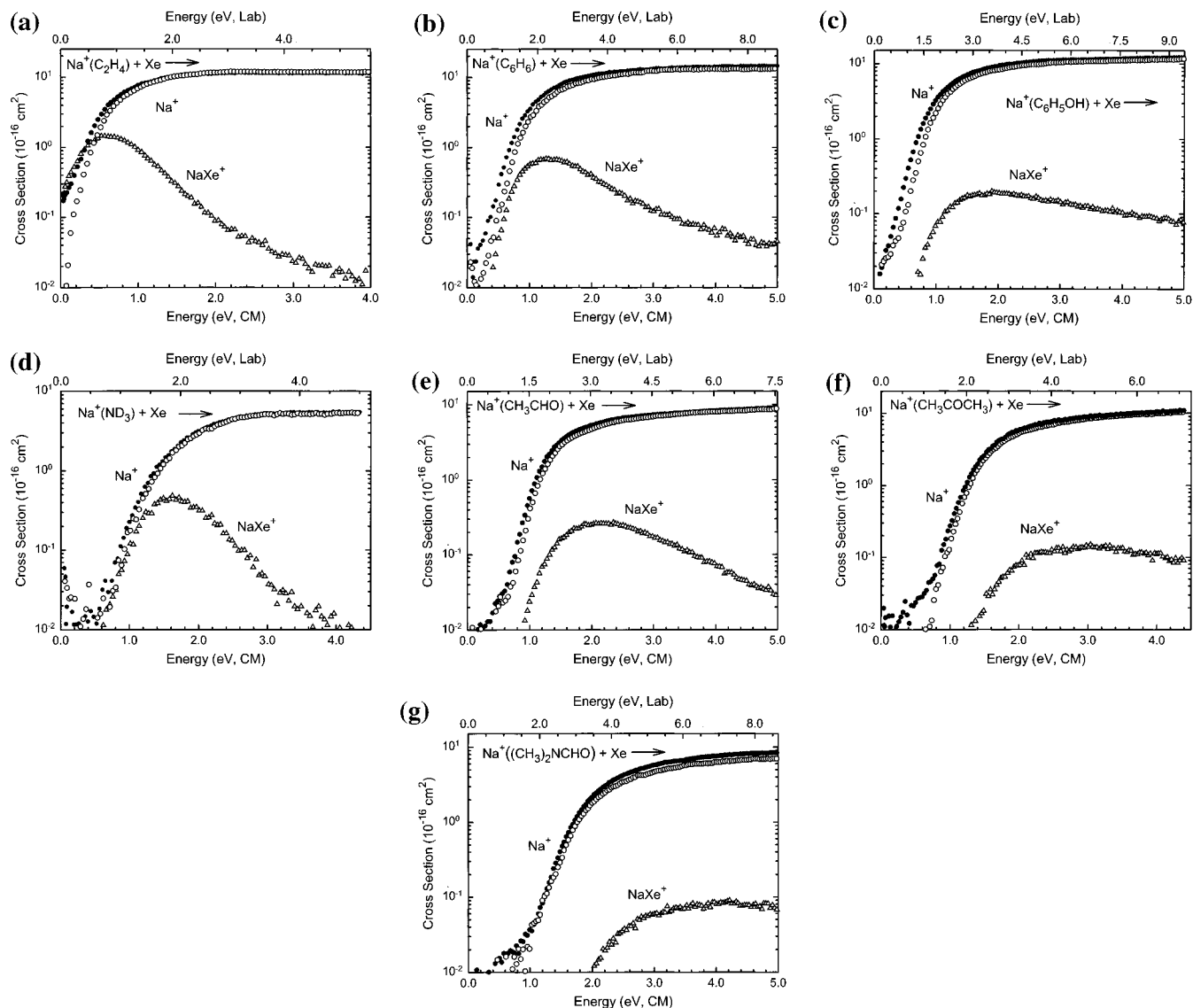


Figure 1. Cross sections for collision-induced dissociation of $\text{Na}^+(\text{L})$ complexes where $\text{L} = \text{C}_2\text{H}_4$, C_6H_6 , $\text{C}_6\text{H}_5\text{OH}$, ND_3 , CH_3CHO , CH_3COCH_3 , and $(\text{CH}_3)_2\text{NCHO}$ (parts a–g, respectively) with Xe as a function of kinetic energy in the center-of-mass frame (lower x-axis) and the laboratory frame (upper x-axis). Data are shown for a xenon pressure of ~ 0.20 mTorr (\bullet) and extrapolated to zero (\circ). Cross sections for the ligand exchange process to form NaXe^+ are also shown (Δ).

TABLE 1: Fitting Parameters of Eq 1, Threshold Dissociation Energies at 0 K, and Entropies of Activation at 1000 K^a

reactant complex	σ_0^b	n^b	E_0^c (eV)	$E_0(\text{PSL})$ (eV)	$\Delta S^\ddagger(\text{PSL})$ ($\text{J mol}^{-1} \text{K}^{-1}$)
$\text{Na}^+(\text{C}_2\text{H}_4)$	12.7 (0.2)	1.4 (0.1)	0.45 (0.05)	0.45 (0.05)	25 (3)
$\text{Na}^+(\text{C}_6\text{H}_6)$	14.3 (1.3)	1.2 (0.1)	0.92 (0.05)	0.92 (0.05)	50 (3)
$\text{Na}^+(\text{C}_6\text{H}_5\text{OH})$	14.9 (1.1)	1.0 (0.1)	1.02 (0.04)	1.02 (0.04)	47 (2)
$\text{Na}^+(\text{ND}_3)$	5.7 (0.2)	1.1 (0.1)	1.08 (0.06)	1.08 (0.06)	26 (3)
$\text{Na}^+(\text{CH}_3\text{CHO})$	10.0 (0.4)	1.1 (0.1)	1.18 (0.04)	1.18 (0.04)	16 (2)
$\text{Na}^+[(\text{CH}_3)_2\text{CO}]$	13.8 (0.3)	1.1 (0.1)	1.38 (0.04)	1.35 (0.04)	17 (3)
$\text{Na}^+[(\text{CH}_3)_2\text{NCHO}]$	9.6 (0.7)	1.1 (0.1)	1.73 (0.03)	1.62 (0.04)	22 (2)

^a Uncertainties are listed in parentheses. ^b Average values for loose PSL transition state. ^c No RRKM analysis.

systems) and cross section magnitudes of at least a factor of 100. The possibility that thresholds are shifted by kinetic effects associated with the lifetimes of the energized molecules was examined using the RRKM analysis with a loose phase space limit (PSL) model for the dissociation transition state.³⁵ Previous work has shown that this model provides the most accurate assessment of the kinetic shifts for CID processes.^{34,35,38,39,51} As indicated in Table 1, kinetic shifts were found to be negligibly small in all systems but those having the highest threshold energies, $\text{Na}^+(\text{acetone})$ and $\text{Na}^+[(\text{CH}_3)_2\text{NCHO}]$ where they are 0.028 and 0.11 eV, respectively. A measure of the

looseness of the TS is given by entropies of activation, ΔS^\ddagger , listed in Table 1 at 1000 K. These entropies of activation can be favorably compared to ΔS^\ddagger_{1000} values in the range 29–46 $\text{J mol}^{-1} \text{K}^{-1}$ collected by Lifshitz for several simple bond cleavage dissociations of ions.⁵² This is reasonable considering that the TS is expected to lie at the centrifugal barrier for association of $\text{Na}^+ + \text{L}$.

Theoretical Results. Structures for CO, ethene, benzene, methanol, dimethyl ether, water, phenol, ethanol, ammonia, methylamine, 1-propanol, 2-propanol, acetaldehyde, acetone, imidazole, *N,N*-dimethylformamide, and dimethoxyethane, and

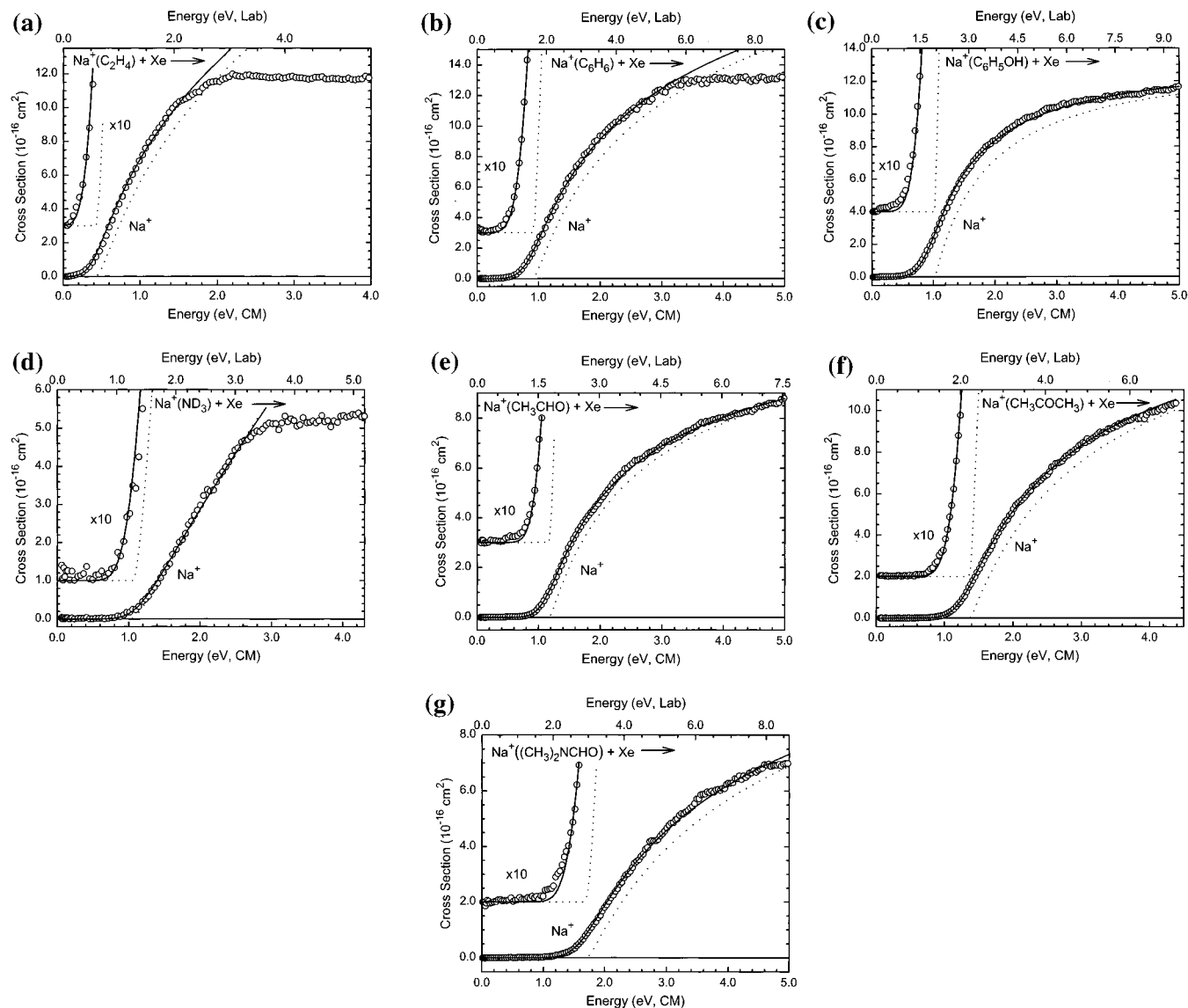


Figure 2. Zero-pressure extrapolated cross sections for collision-induced dissociation of $\text{Na}^+(\text{L})$ complexes where $\text{L} = \text{C}_2\text{H}_4$, C_6H_6 , $\text{C}_6\text{H}_5\text{OH}$, ND_3 , CH_3CHO , CH_3COCH_3 , and $(\text{CH}_3)_2\text{NCHO}$ (parts a–g, respectively) with Xe in the threshold region as a function of kinetic energy in the center-of-mass frame (lower x-axis) and the laboratory frame (upper x-axis). Solid lines show the best fits to the data using the model of eq 1 convoluted over the neutral and ion kinetic and internal energy distributions. Dotted lines show the model cross sections in the absence of experimental kinetic energy broadening for reactants with an internal energy of 0 K.

for the complexes of Na^+ with all of these species and Ar were calculated as described above. Table 2 gives details of the final geometries for each of these species. Results for the most stable conformations of the sodium ion–ligand complexes studied experimentally are shown in Figures 3 and 4. The π -complexes with ethene and benzene place the sodium cation in the most symmetric position yielding complexes with C_{2V} and C_{6V} symmetry, respectively. There is little distortion of the ligand in the case of the ethene complex, while the C–C bonds expand by about 0.008 Å upon complexation of benzene to Na^+ . In agreement with the results of Hoyau et al.,¹ we find two stable minima for the $\text{Na}^+(\text{phenol})$ complex. The ground state, shown in Figure 3, has the sodium cation bound to the benzene ring although displaced from the center because of the influence of the hydroxy group. Here, too, the C–C bonds expand upon complexation, the C–O bond lengthens by 0.018 Å, and the OH rotates by 12° out of the plane of the aromatic ring. The low-lying excited conformation has the sodium bound to the oxygen atom but still above the plane of the ligand. Here, the aromatic ring remains largely unperturbed upon complexation,

but the CO bond expands by 0.034 Å, the OH bond by only 0.003 Å, and the OH rotates by 32° out of the plane of the aromatic ring. At the MP2 level of theory (including separate zero-point energy and BSSE corrections), we find that the 0 K binding energy for this second geometry is 4.4 kJ/mol less than the ground state. Figure 4 shows that the sodium cation binds to the nitrogen lone-pair electrons in ammonia and to the oxygen lone-pair electrons in the carbonyl group of the aldehyde, formamide, and ketone. In these cases, the distortion of the ligand upon sodium ion binding is very small.

Sodium ion binding energies were determined using the MP2-(full)/6-31G* geometries and single-point energy calculations performed at the MP2(full)/6-311+G(2d,2p) level. Values corrected for zero-point energies and BSSE^{53–55} are listed in Table 3 for the ground state. Over half of these values have been previously calculated by Hoyau et al.¹ To evaluate the accuracy of comparable calculations using density functional theory, we also calculated BDEs using B3LYP/6-31G* geometries with single-point energy calculations at the B3LYP/6-311+G(2d,2p) level including BSSE corrections and comparable

TABLE 2: MP2(full)/6-31G* Geometry Optimized Structures of the Na⁺(L) Complexes^a

L	symmetry	Na ⁺ -X distance (Å)	Na ⁺ -X-Y angle (°)
Ar	C _{∞v}	2.814	
CO	C _{∞v}	2.597	180.0
C ₂ H ₄	C _{2v}	2.745	75.8
C ₆ H ₆	C _{6v}	2.757	75.3
CH ₃ OH	C _s	2.209	129.3
CH ₃ OCH ₃	C _{2v}	2.207	124.7
H ₂ O	C _{2v}	2.220	127.6
C ₆ H ₅ OH (geom 1) ^b	C ₁	2.835 (C1)	78.1 (C2), 76.8 (C6)
C ₆ H ₅ OH (geom 2) ^b	C ₁	2.255 (O)	92.3 (C1)
C ₂ H ₅ OH	C _s	2.203	120.9
NH ₃	C _{3v}	2.366	113.6
CH ₃ NH ₂	C _s	2.367	115.0
1-C ₃ H ₇ OH	C _s	2.202	118.6
2-C ₃ H ₇ OH	C ₁	2.198	120.8
CH ₃ CHO	C _s	2.167	174.1
CH ₃ COCH ₃	C _{2v}	2.147	180.0
imidazole	C _s	2.312	130.0 (C2), 124.5 (C5)
(CH ₃) ₂ NCHO	C _s	2.109	161.2
(CH ₃ OCH ₂) ₂	C ₂	2.260	129.6 (C1), 110.1 (C3)

^a X is the atom in the ligand closest to the sodium cation; Y is the heaviest atom bonded to X. ^b Relative energies: 0.0 for geometry 1 and 4.4 kJ/mol for geometry 2.

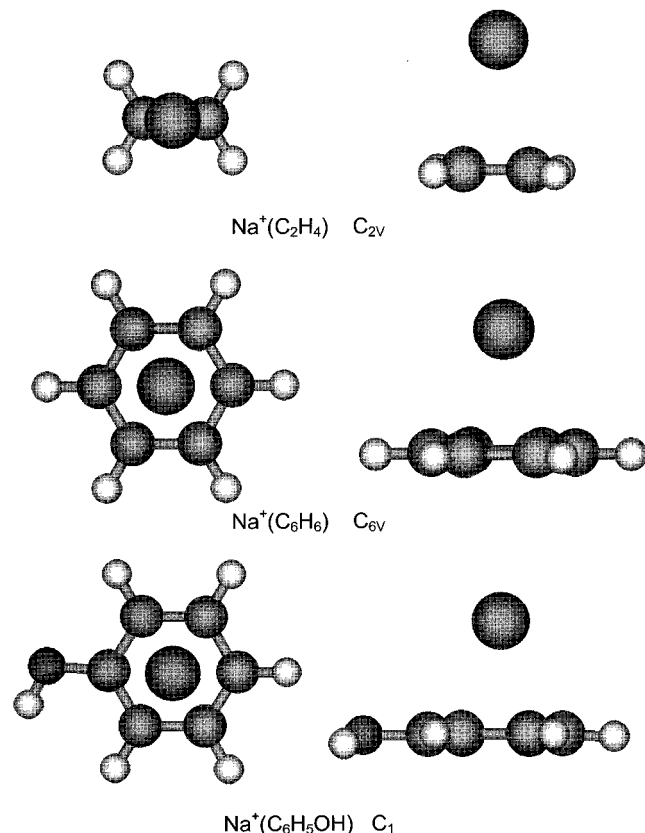


Figure 3. Ground-state geometries of Na⁺(L) where L = C₂H₄, C₆H₆, and C₆H₅OH, showing views from the side and above, optimized at the MP2(full)/6-31G* level of theory.

calculations using the B3P86 hybrid functional. Zero-point energy corrections used scaled frequencies from the MP2 calculations. For comparison, this table also lists dissociation energies calculated for these species using the complete basis set extrapolation protocols, CBS-4, CBS-4M, and CBS-Q,¹⁹ and the G2 and G3 methods.^{16,17} (G2 calculations on the two largest complexes, those with phenol and dimethoxyethane, were beyond our computational resources. The present G2 calcula-

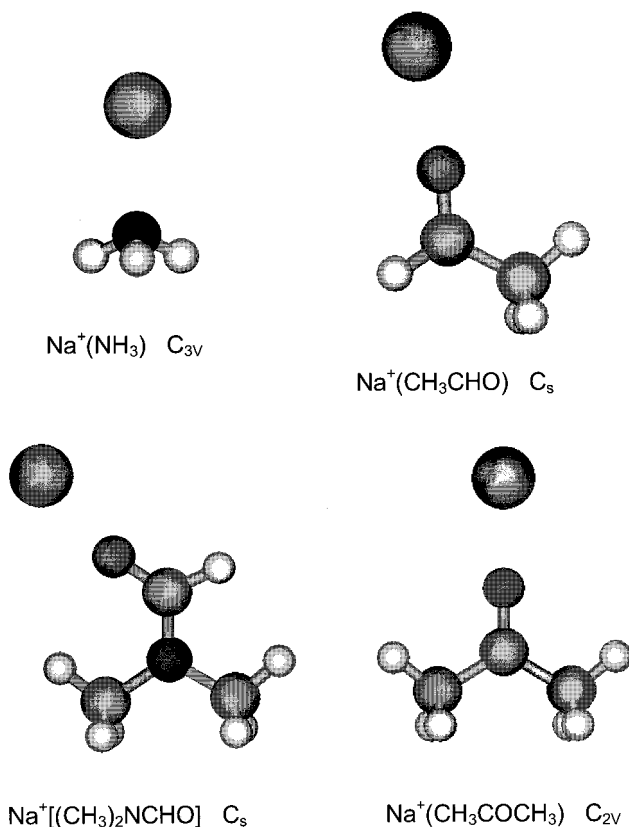


Figure 4. Ground-state geometries of Na⁺(L) where L = ND₃, CH₃CHO, CH₃COCH₃, and (CH₃)₂NCHO optimized at the MP2(full)/6-31G* level of theory.

tions on the CH₃OH, H₂O, NH₃, CH₃NH₂, and CH₃CHO complexes reproduce previous G2 calculations by Remko and Sarrisky^{56,57} and Remko.^{57,58} These five methods are compound methodologies designed to provide high-accuracy energies. They (excluding CBS-4M) have been found to have mean average deviations (MAD) of 8.4, 4.2, 5.0, and 4.3 kJ/mol, respectively, for the G2 test set of thermodynamic values.^{17,43}

A comparison of the various theoretical results for the 18 complexes included here is shown in Figure 5. (This figure excludes CBS-4M results to avoid overcrowding and G3 results because there are fewer values available for comparison.) It is clear that the general trends among all levels of theory are the same. Generally, the B3LYP values are the highest and often the CBS-4 values are the lowest. CBS-4M results are very similar to CBS-4 results, as might be expected, but are larger by an average of 0.7 kJ/mol. In contrast, G3 theory does not agree very well with G2 theory and yields values an average of 9.3 kJ/mol higher, comparable or higher than the B3LYP values. CBS-Q theory, which on the basis of the G2 test set comparisons is arguably the highest level of theory used, generally provides a central value. It can also be noted, however, that the agreement between the CBS-Q, MP2, and B3P86 levels of theory is quite good. There is one anomalous value in all the calculations: G2 for Na⁺(imidazole), shown in Figure 5. Because of the complexities of this compound theoretical model, it is difficult to isolate where the breakdown in this calculation has occurred. The geometries calculated at the different levels of theory are comparable to one another in this case.

Discussion

Comparison between Theory and Experiment. The sodium cation affinities of several molecules at 0 K measured by guided

TABLE 3: Experimental and Calculated Na⁺-L Binding Enthalpies at 0 K (in kJ/mol)

ligand	experiment		theory							
	GIBMS	literature ^a	MP2	B3LYP	B3P86	CBS-4	CBS-4M	CBS-Q	G2	G3
Ar	15.4 (8.7)		10.9	13.7	10.9	8.4	7.5	12.0	14.4	21.6
CO	31.8 (7.7)	50.8 ^b	39.7	39.0	36.0	34.3	33.5	36.3	43.1	43.4
C ₂ H ₄	43.1 (4.4)		51.4 ^c	57.3	54.2	49.8	50.6	46.0	51.7	59.7
C ₆ H ₆	88.3 (4.3)	115.5 (6.3) ^d	89.4 ^c	94.9	92.2	92.4	94.6	90.9	94.4	
CH ₃ OH	91.7 (5.7)	109.8 (0.8) ^e 98.9 (0.8) ^g	100.0 ^c	105.2	100.8	92.9	93.9	96.2	98.5 ^f	109.2
CH ₃ OCH ₃	91.7 (4.8)		101.7 ^c	105.5	100.8	93.9	94.8	101.0	100.3	111.8
H ₂ O	94.6 (7.5)	84 (18) ^h 96.9 ⁱ 97.5 (10) ^j	89.2 ^c	94.6	91.1	85.1	85.9	88.8	88.8 ^f	98.4
C ₆ H ₅ OH	98.5 (3.4)		91.1 ^c	95.8	95.3	100.3	96.3	101.9		
C ₂ H ₅ OH	102.0 (3.7)		108.9	114.7	111.1	101.0	102.2	104.4	107.6	120.8
NH ₃	102.2 (5.4)	117.8 (1.7) ^k 103.1 (0.8) ^g 115 (18) ^h	102.5 ^c	108.7	105.4	103.8	103.8	96.7	102.2 ^f	112.0
CH ₃ NH ₂		132.0 ^e 107.7 (0.8) ^g	108.7 ^c	115.2	111.2	106.7	106.6	105.9	108.2 ^f	118.7
1-C ₃ H ₇ OH	108.0 (4.1)		112.0	115.1	111.0	104.3	105.6	108.7	103.3	
2-C ₃ H ₇ OH	113.2 (4.3)	123.1 ^l	113.0	119.5	115.6	105.4	106.6	117.0	103.7	
CH ₃ CHO	113.4 (3.4)		112.1	123.3	118.9	107.0	108.3	115.7	114.0 ^m	124.4
CH ₃ COCH ₃	130.5 (4.1)	138.9 (0.8) ^e 128.1 (2.1) ^g 137.7 ^l	124.9 ^c	137.3	133.3	120.0	122.0	127.1	126.9	138.3
imidazole	139.7 (5.2)		144.0 ^c	151.9	147.5	140.4	141.0	144.8	119.6	
(CH ₃) ₂ NCHO	156.7 (3.7)	150.4 ^l	154.0 ^c	163.5	157.8	147.6	149.9	153.6	155.2	
(CH ₃ OCH ₂) ₂	158.2 (3.9)	195.8 ^b	167.1	174.9	167.7	152.1	153.9	165.1		
mean	This work (17 values)		5.1 (3.2)	8.5 (4.7)	5.5 (3.1)	4.8 (3.2)	4.5 (2.8)	4.8 (3.2)	5.3 (3.6) ⁿ	12.3 (4.5)
absolute deviation	Castleman ^{b,d,e,k} (7 values)		18 (8)	11 (8)	16 (9)	22 (11)	22 (10)	22 (11)	14 (5)	6 (5)
	Hoyau et al. ^g (4 values)		1.5 (1.2)	7.2 (1.6)	3.2 (1.5)	4.0 (3.7)	3.2 (2.7)	4.0 (3.7)	0.8 (0.4)	10.4 (1.0)

^a All literature values adjusted to 0 K. ^b Ref 10. ^c These values reproduce results of Hoyau et al.¹ ^d Ref 15. ^e Ref 4. ^f These values reproduce results of ref 56. ^g Ref 1. ^h Ref 3. ⁱ Ref 13. ^j Ref 14. ^k Ref 2. ^l Ref 5. ^m These values reproduce results of ref 57. ⁿ Excluding value for imidazole.

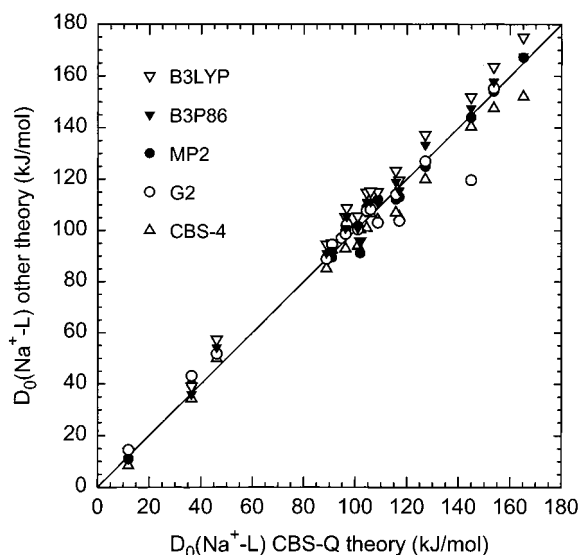


Figure 5. Ab initio calculated bond dissociation energies (in kJ/mol) for Na⁺-L where L includes all 18 ligands listed in Table 3. All values are at 0 K and are taken from Table 3. The plot shows results from B3LYP (▽), B3P86 (▼), MP2 (●), G2 (○), and CBS-4 (△) calculations vs those from CBS-Q calculations. The diagonal line has a slope of unity.

ion beam mass spectrometry and calculated here are summarized in Table 3. The agreement between theory and experiment is generally very good. The mean absolute deviation (MAD) between experiment and the MP2 theory values for the 17 systems considered is 5.1 ± 3.2 kJ/mol (and a mean deviation of 1.9 ± 5.8 kJ/mol). This is comparable to the average experimental error of 5.0 ± 1.6 kJ/mol and well within expected computational accuracy (about 8 kJ/mol). In contrast, the B3LYP

theory values are consistently too high, with a MAD from our experiments of 8.5 ± 4.7 kJ/mol (and a mean deviation of 8.0 ± 5.6 kJ/mol). For the purposes of obtaining thermochemistry on these sodium cation complexes, the B3P86 hybrid functional performs better, with a MAD from experiment of 5.5 ± 3.1 kJ/mol (and a mean deviation of 4.2 ± 4.8 kJ/mol), comparable to the MP2 calculations.

Ostensibly, one expects that the compound methods (CBS-4, CBS-4M, CBS-Q, G2, and G3) should provide better agreement with experiment as these methods are designed to provide accurate energetics. However, none of these methods was explicitly tested or developed with complexes such as those studied here in mind and indeed the G2 test set of molecules does not include ring compounds of any sort. Nevertheless, if we compare our experimental values to results of the CBS-4 calculations, the MAD is 4.8 ± 3.3 kJ/mol, comparable to the MP2 deviation. The mean deviation (theory - exp.) of -2.8 ± 5.3 kJ/mol shows that the CBS-4 calculations generally fall below the experimental values. The CBS-4M model improves the agreement slightly with a MAD of 4.5 ± 2.8 kJ/mol and a mean deviation (theory - exp.) of -1.7 ± 5.2 kJ/mol. The highest levels of theory, CBS-Q and G2 (excluding imidazole), have MADs from our experimental values of 4.1 ± 2.0 and 5.3 ± 3.6 kJ/mol, respectively. The mean deviations of 1.6 ± 4.4 and 1.5 ± 6.3 kJ/mol, respectively, illustrate that these values are scattered fairly evenly above and below the experimental values. The performance of the "improved" G3 theory is disappointing, with a MAD of 12.3 ± 5.6 kJ/mol and an identical mean deviation as all values are systematically higher than experiment.

The overall agreement between CBS-Q theory and our experimental results is shown in Figure 6. It can be seen that the agreement is excellent over the order-of-magnitude range

TABLE 4: Enthalpies and Free Energies of Na^+-L at 0 and 298 K (in kJ/mol)^a

system	ΔH_0^b	$\Delta H_{298} - \Delta H_0^c$	ΔH_{298}	$T\Delta S_{298}^c$	ΔG_{298}
$\text{Na}^+(\text{Ar})$	15.4 (8.7)	1.9 (0.1)	17.3 (8.7)	18.2 (0.2)	-0.9 (8.7)
$\text{Na}^+(\text{CO})$	31.8 (7.7)	1.5 (0.2)	33.3 (7.7)	32.2 (0.5)	1.1 (7.7)
$\text{Na}^+(\text{C}_2\text{H}_4)$	43.1 (4.4)	1.5 (0.2)	44.6 (4.4)	25.0 (0.5)	19.6 (4.4)
$\text{Na}^+(\text{C}_6\text{H}_6)$	88.3 (4.3)	1.7 (0.2)	90.0 (4.3)	30.7 (0.5)	59.3 (4.3)
$\text{Na}^+(\text{CH}_3\text{OH})$	91.7 (5.7)	1.5 (0.2)	93.2 (5.7)	27.5 (0.5)	65.7 (5.7)
$\text{Na}^+(\text{CH}_3\text{OCH}_3)$	91.7 (4.8)	0.9 (0.2)	92.6 (4.8)	26.2 (0.5)	66.4 (4.8)
$\text{Na}^+(\text{H}_2\text{O})$	94.6 (7.5)	3.5 (0.3)	98.1 (7.5)	23.7 (0.3)	74.4 (7.5)
$\text{Na}^+(\text{C}_6\text{H}_5\text{OH})$	98.5 (3.4)	1.8 (0.2)	100.3 (3.4)	30.6 (0.4)	69.7 (3.4)
$\text{Na}^+(\text{C}_2\text{H}_5\text{OH})$	102.0 (3.7)	1.3 (0.2)	103.3 (3.7)	28.0 (0.5)	75.3 (3.7)
$\text{Na}^+(\text{NH}_3)$	102.2 (5.4)	4.0 (0.3)	106.2 (5.4)	24.8 (0.2)	81.4 (5.4)
$\text{Na}^+(\text{ND}_3)$	103.9 (5.4)	3.3 (0.3)	107.2 (5.4)	25.9 (0.3)	81.3 (5.4)
$\text{Na}^+(\text{CH}_3\text{NH}_2)$	108.6 (0.8)	2.3 (0.2)	110.9 (0.8) ^d	26.6 (0.4)	84.3 (0.9)
$\text{Na}^+(1-\text{C}_3\text{H}_7\text{OH})$	108.0 (4.1)	1.3 (0.2)	109.3 (4.1)	28.9 (0.6)	80.4 (4.1)
$\text{Na}^+(2-\text{C}_3\text{H}_7\text{OH})$	113.2 (4.3)	1.2 (0.2)	114.4 (4.3)	28.9 (0.6)	85.5 (4.3)
$\text{Na}^+(\text{CH}_3\text{CHO})$	113.4 (3.4)	1.0 (0.2)	114.4 (3.4)	25.7 (0.5)	88.7 (3.4)
$\text{Na}^+[\text{OC}(\text{CH}_3)_2]$	130.5 (4.1)	0.8 (0.1)	131.3 (4.1)	25.6 (0.5)	105.7 (4.1)
$\text{Na}^+(\text{imidazole})$	139.7 (5.2)	1.2 (0.2)	140.9 (5.2)	27.6 (0.5)	113.3 (5.2)
$\text{Na}^+[(\text{CH}_3)_2\text{NCHO}]$	156.7 (3.7)	1.1 (0.2)	157.8 (3.7)	27.2 (0.5)	130.6 (3.7)
$\text{Na}^+[(\text{CH}_3\text{OCH}_2)_2]$	158.2 (3.9)	1.7 (0.3)	159.9 (3.9)	31.2 (0.5)	128.7 (3.9)

^a Uncertainties are listed in parentheses. ^b Experimental values from this work except for CH_3NH_2 ; taken from Table 3. ^c Calculated using standard formulas and molecular constants calculated at the MP2(full)/6-31G* level. For experimentally studied complexes, the molecular constants are given in Tables 1S and 2S. Uncertainties correspond to 10% variations in the vibrational frequencies. ^d Hoyau et al. (ref 1).

spanned by these results. Indeed, a linear regression analysis of this comparison yields an intercept of 1.1 kJ/mol and a slope of 1.005, indicating that this level of theory reproduces the experimental results with high fidelity. Similar comparisons with the other levels of theory provide slightly less favorable results in all cases (excluding the anomalous imidazole result for G2 theory). Given this observation, the relative MAD values, the failure of G2 theory for imidazole, and the poor performance of G3 theory, CBS-Q theory provides the highest level of agreement with experiment, is reliable, and computationally less intensive than G2 and G3 theories. Both the MP2 and B3P86 calculations give fairly reliable results at a reasonable computational cost. (Comparisons with our experimental results give linear correlations having intercepts of 3.4 and 2.0 kJ/mol and slopes of 0.986 and 1.022, respectively.) B3LYP and G3 clearly overestimate the bonding for sodium cation binding affinities. CBS-4 theory tends to underestimate the bond energies slightly, and CBS-4M reduces this underestimation.

Conversion from 0 to 298 K. To allow comparison to previous literature values and commonly used experimental conditions, we convert the 0 K bond energies determined here to 298 K bond enthalpies and free energies. The enthalpy conversions are calculated using standard formulas and the vibrational and rotational constants determined using MP2(full)/6-31G* calculations, such as those given in Tables S1 and S2. Table 4 lists 0 and 298 K enthalpy, free energy, and enthalpic and entropic corrections for all systems experimentally determined. Uncertainties in these values are determined by 10% variations in the molecular constants. It should be noted that somewhat different ΔS_{298} values are obtained by other theoretical calculations and in some cases our values differ somewhat from those provided by Hoyau et al.¹ Using these values, we have adjusted enthalpy values taken from the literature (invariably listed at 298 K) to 0 K. These are compared to the present results in Table 3 and Figure 6.

Comparison with Literature Values. Comparison of the present results with the experimental results of Hoyau et al.¹ for the three systems that overlap, methanol, ammonia, and acetone, finds good agreement, as can be seen in Figure 6. The ammonia and acetone binding energies are in very good agreement, well within experimental error. The values for methanol disagree slightly more, as has been discussed in more

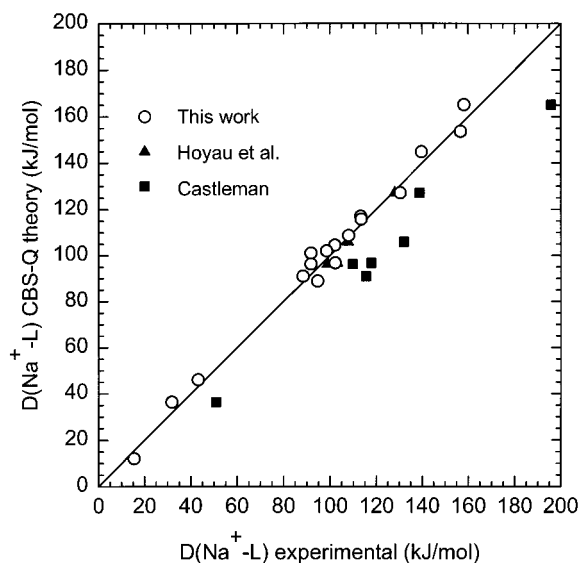


Figure 6. Theoretical vs experimental bond dissociation energies (in kJ/mol) for Na^+-L where L includes all 18 ligands listed in Table 3. All values are at 0 K and are taken from Table 3. Theory is represented by results from CBS-Q calculations. Experimental results include those from the present work (○), from Hoyau et al. (▲, ref 1) and from Castleman and co-workers (■, refs 2, 4, 10, and 15). The diagonal line indicates the values for which calculated and measured bond dissociation energies are equal.

detail elsewhere.⁷ There, we concluded that a value near the upper end of our experimental range is likely to be the most accurate. Comparison of the four experimental values from Hoyau et al.¹ with the various theories shows good agreement. Theory and experiment have MADs ranging from 0.8 ± 0.4 kJ/mol for G2 theory to 10.4 ± 1.0 kJ/mol for G3 calculations.

The most extensive set of experimental values for Na^+ bond energies to various molecules comes from equilibrium studies of Castleman and co-workers.^{2,4,10,15} For the six systems studied both here and by Castleman, the mean deviation (and MAD) between these results and ours is 21 ± 10 kJ/mol. As can be seen in Figure 6, the Castleman numbers are systematically higher than the present values. We can also compare these other experimental values with the theoretical results calculated here. For the seven values from Castleman and co-workers,^{2,4,10,15}

the MADs range from 6 ± 5 kJ/mol for the G3 calculations up to 22 ± 11 kJ/mol for the CBS-4 calculations. In all cases, the theoretical values lie below the values from Castleman and co-workers, clearly not supporting the higher values. It appears that these experiments systematically overestimate the bonding for reasons that are not clear.

Results from Feng and Gronert⁵ for 2-C₃H₇OH and (CH₃)₂-CO are also higher than the present results, while that for (CH₃)₂-NCHO is somewhat lower. These differences may occur because these kinetic method results were anchored to a value for *N,N*-dimethylacetamide from the CID studies of Klassen et al.⁶ As *N,N*-dimethylformamide is a chemically similar molecule, while acetone and propanol are not, perhaps it is not surprising that the kinetic method yields an accurate value only for the former complex.

For the complexes studied here, there are only two other systems for which experimental values previously exist. Early CID results from Marinelli and Squires³ provided Na⁺ binding affinities to water and ammonia. Within the large experimental uncertainties, these results are in good agreement with experiment and theory although it seems odd that their number for water is fairly low compared to the other results, while that for ammonia is nearly as high as that from Castleman's work. The remaining experimental values are for the Na⁺(H₂O) complex and come from the early equilibrium studies of Dzidic and Kebarle¹³ (where no error estimate was provided) and the flame studies of Burdett and Hayhurst.¹⁴ These values are within experimental error of our previous CID measurement,¹¹ but are about 8 kJ/mol higher than the best theoretical values.

We have not included a detailed discussion of previous theoretical results for these complexes. Such results have been summarized and discussed thoroughly by Hoyau et al.¹ and the reader is referred to this paper for such a comparison.

Qualitative Trends. Examination of the experimental and theoretical BDEs given in Table 3 yields some expected trends and some interesting results. Not surprisingly, the sole rare gas, Ar, in this list is the most weakly bound ligand. The most strongly bound ligand, (CH₃OCH₂)₂, is the only bidentate species. Species forming π -complexes, C₂H₄, C₆H₆, and C₆H₅-OH, are less strongly bound than ligands having lone pairs. This is also illustrated by the optimal position for binding in the systems containing a carbonyl, i.e., CH₃CHO, CH₃COCH₃, and (CH₃)₂NCHO, Figure 4. Given this conclusion, the phenol ligand provides an interesting dichotomy as it prefers to bind to the benzene π -cloud rather than the lone-pair electrons of the oxygen atom. Certainly, the measured bond energies for benzene and methanol (Table 3) suggest that the lone-pair site should be slightly favored. However, we note that complexation at the oxygen site disrupts the electron delocalization that helps stabilize the free phenol ligand. This disruption induces a rotation of the OH group out of the plane of the aromatic ring by 32° (see above), while in the π -complex, much less distortion occurs (12° rotation). Calculations on the distorted ligands indicate that this destabilization costs about 8.2 kJ/mol for the oxygen-bound species (geometry 2) while the energetic cost is only 3.7 kJ/mol for the π -complex (geometry 1). This difference inverts the relative stabilities of the lone-pair vs π -complex geometries.

It is also interesting to note that species such as NH₃ and CH₃NH₂ bind more strongly to Na⁺ than the analogous ligands, H₂O and CH₃OH, which is somewhat surprising as the latter species have larger dipole moments⁵⁹ and shorter metal–ligand bond distances (Table 2). In related studies,⁶⁰ theory has pointed out that in such complexes the effective position of the ammonia

dipole is closer to the metal ion than the M–N bond distance, while the effective position of the water dipole is slightly farther away than the M–O bond distance. This difference leads to a strong electrostatic interaction in the former case. It should be realized that this comparison cannot be generalized to all nitrogen- vs oxygen-based ligands as binding to CH₃CHO is greater than to CH₃NH₂. Presumably, this can be rationalized on the basis of the larger dipole moment and closer bond distance for the former ligand. Overall, these results suggest that there are several factors that influence the strength of Na⁺ binding which include the nature of the donor atom, the localization of the electron density on the donor (orbital overlap with the metal ion), electrostatic interactions (polarizability, charge-dipole, and charge-quadrupole), and the possibility for multiple donor (chelation) interactions.

One place where additional experiments seem warranted is illustrated by examining trends in the bonding as methyl groups are substituted for H atoms. In the case of a carbonyl, such a substitution (CH₃CHO \rightarrow CH₃COCH₃) yields a large increase, 17 ± 5 kJ/mol (experiment) or about 13 kJ/mol (theory). In contrast, such a substitution at the N atom of ammonia (NH₃ \rightarrow CH₃NH₂) increases the binding by only 5 ± 1 kJ/mol (experiment) or about 6 kJ/mol (theory). A slightly larger increase, 7.4–10.8 kJ/mol, is predicted by theory for the substitution at the O atom of water (H₂O \rightarrow CH₃OH), while our experimental results are inverted. This is additional evidence that the Na⁺(CH₃OH) bond energy is closer to our upper limit or the 98.9 kJ/mol value measured in equilibrium studies by Hoyau et al.¹ Note, however, that this latter result for Na⁺(CH₃-OH) is only 2 kJ/mol above the value for Na⁺(H₂O) measured in equilibrium studies by Dzidic and Kebarle¹³ or by flame mass spectrometry by Burdett and Hayhurst.¹⁴ This suggests that this latter value is too high, in agreement with our results and theory. If another methyl group substitution is made (CH₃OH \rightarrow CH₃-OCH₃), theory predicts a small energy change of 0.0–4.8 kJ/mol, in agreement with our experimentally determined relative values. However, if the Na⁺(CH₃OH) BDE is revised upward, then the absolute BDE for Na⁺(CH₃OCH₃) may also lie toward the upper end of our experimental range. In these comparisons, it should be realized that the threshold CID measurements are completely independent of one another with uncertainties representative of the absolute values, rather than of systematic and relative errors. Clearly, experiments designed to more precisely determine the relative values of the water to methanol to dimethyl ether sequence would be of interest. Likewise (as noted previously), such experiments comparing the relative values of 1- and 2-propanol would be of interest as experiment yields a difference of 5 kJ/mol while theory predicts differences ranging from 0.7 to 8.3 kJ/mol (with the extremes given by the two highest levels of theory).

Conclusions

The kinetic energy dependencies of the collision-induced dissociations of Na⁺(L), L = ethene, benzene, phenol, ammonia, acetaldehyde, acetone, and *N,N*-dimethylformamide with Xe, are examined in a guided ion beam mass spectrometer. The dominant dissociation process in all cases is formation of Na⁺ + L. Thresholds at 0 K for these processes are determined after consideration of the effects of reactant internal energy, multiple collisions with Xe, and lifetime effects using a phase space limit transition state model. Our experimental results agree well with high-pressure mass spectrometry experiments of Hoyau et al.¹ but not with those of Castleman and co-workers.^{2,4,10,15} Values reported here for ethene, acetaldehyde,

and phenol constitute the first experimental determinations of the sodium cation binding affinities. Combined with the experimental results of Hoyau et al., these values comprise a set of reliable anchors for a sodium cation affinity scale that cover a wide range of binding affinities. This conclusion is confirmed by good agreement with *ab initio* calculations at several levels of theory. Further, these calculations establish that CBS-Q theory provides excellent values for comparison with theory, while values computed at the MP2 or B3P86 levels of theory (6-31G* basis for geometries and 6-311+G(2d,2p) basis for single-point energy calculations) including zero-point and BSSE corrections yield reasonable results at lower computational cost. Such calculations, as performed here and by Hoyau et al., can extend the sodium cation affinity scale to other molecules reliably.

Acknowledgment. Funding for this work was provided by the National Science Foundation under Grant CHE-9877162. We thank Gilles Ohanessian and Terry McMahon for providing a copy of their work prior to publication and for personal communications regarding their studies.

Supporting Information Available: Tables of vibrational frequencies and average vibrational energies at 298 K and rotational constants of Na⁺(L) in cm⁻¹. This material is available free of charge via the Internet at <http://pubs.acs.org>.

References and Notes

- Hoyau, S.; Norrman, K.; McMahon, T. B.; Ohanessian, G. *J. Am. Chem. Soc.*, accepted for publication.
- Castleman, A. W.; Holland, P. M.; Lindsay, D. M.; Peterson, K. I. *J. Am. Chem. Soc.* **1978**, *100*, 6039.
- Marinelli, P. J.; Squires, R. R. *J. Am. Chem. Soc.* **1989**, *111*, 4101.
- Guo, B. C.; Conklin, B. J.; Castleman, A. W. *J. Am. Chem. Soc.* **1989**, *111*, 6506.
- Feng, W. Y.; Gronert, S. Unpublished data.
- Klassen, J. S.; Anderson, S. G.; Blades, A. T.; Kebarle, P. *J. Phys. Chem.* **1996**, *100*, 14218.
- Rodgers, M. T.; Armentrout, P. B. *J. Phys. Chem. A* **1999**, *103*, 4955.
- Walter, D.; Sievers, M. R.; Armentrout, P. B. *Int. J. Mass Spectrom.* **1998**, *173*, 93.
- More, M. B.; Ray, D.; Armentrout, P. B. *J. Phys. Chem. A* **1997**, *101*, 831.
- Castleman, A. W.; Peterson, K. I.; Upschulte, B. L.; Schelling, F. *J. Int. J. Mass Spectrom. Ion Processes* **1983**, *47*, 203.
- Dalleska, N. F.; Tjelta, B. L.; Armentrout, P. B. *J. Phys. Chem.* **1994**, *98*, 4191.
- Rodgers, M. T.; Armentrout, P. B. *Int. J. Mass Spectrom.* **1999**, *185–187*, 359.
- Dzidic, I.; Kebarle, P. *J. Phys. Chem.* **1970**, *74*, 1466.
- Burdett, N. A.; Hayhurst, A. N. *J. Chem. Soc., Faraday Trans. 1* **1982**, *78*, 2997.
- Guo, B. C.; Purnell, J. W.; Castleman, A. W. *Chem. Phys. Lett.* **1990**, *168*, 155.
- Curtiss, L. A.; Raghavachari, K.; Trucks, G. W.; Pople, J. A. *J. Chem. Phys.* **1991**, *94*, 7221.
- Curtiss, L. A.; Raghavachari, K.; Redfern, P. C.; Rassolov, V.; Pople, J. A. *J. Chem. Phys.* **1998**, *109*, 7764.
- Nyden, M. R.; Petersson, G. A. *J. Chem. Phys.* **1981**, *75*, 1843; Petersson, G. A.; Al-Laham, M. A. *J. Chem. Phys.* **1991**, *94*, 6081; Petersson, G. A.; Tensfeldt, T.; Montgomery, J. A. *J. Chem. Phys.* **1991**, *94*, 6091; Montgomery, J. A.; Ochterski, J. W.; Petersson, G. A. *J. Chem. Phys.* **1994**, *101*, 5900.
- Ochterski, J. W.; Petersson, G. A.; Montgomery, J. A. *J. Chem. Phys.* **1996**, *104*, 2598.
- Ervin, K. M.; Armentrout, P. B. *J. Chem. Phys.* **1985**, *83*, 166.
- Schultz, R. H.; Armentrout, P. B. *Int. J. Mass Spectrom. Ion Processes* **1991**, *107*, 29.
- Teloy, E.; Gerlich, D. *Chem. Phys.* **1974**, *4*, 417.; Gerlich, D. Diplomarbeit, University of Freiburg, Federal Republic of Germany, 1971. Gerlich, D., In *State-Selected and State-to-State Ion–Molecule Reaction Dynamics, Part I, Experiment*; Ng, C.-Y., Baer, M., Eds.; *Adv. Chem. Phys.* **1992**, *82*, 1.
- Aristov, N.; Armentrout, P. B. *J. Phys. Chem.* **1986**, *90*, 5135.
- Hales, D. A.; Armentrout, P. B. *J. Cluster Science* **1990**, *1*, 127.
- Armentrout, P. B. In *Advances in Gas-Phase Ion Chemistry*; Adams, N. G., Babcock, L. M., Eds.; JAI: Greenwich, 1992; Vol. 1, pp 83–119.
- Dalleska, N. F.; Honma, K.; Sunderlin, L. S.; Armentrout, P. B. *J. Am. Chem. Soc.* **1994**, *116*, 3519.
- Schultz, R. H.; Crellin, K. C.; Armentrout, P. B. *J. Am. Chem. Soc.* **1992**, *113*, 8590.
- Dalleska, N. F.; Honma, K.; Armentrout, P. B. *J. Am. Chem. Soc.* **1993**, *115*, 12125.
- Khan, F. A.; Clemmer, D. C.; Schultz, R. H.; Armentrout, P. B. *J. Phys. Chem.* **1993**, *97*, 7978.
- Schultz, R. H.; Armentrout, P. B. *J. Chem. Phys.* **1992**, *96*, 1046.
- Fisher, E. R.; Kickel, B. L.; Armentrout, P. B. *J. Phys. Chem.* **1993**, *97*, 10204.
- Beyer, T. S.; Swinehart, D. F. *Comm. Assoc. Comput. Machines* **1973**, *16*, 379. Stein, S. E.; Rabinovitch, B. S. *J. Chem. Phys.* **1973**, *58*, 2438.; *Chem. Phys. Lett.* **1977**, *49*, 1883.
- Pople, J. A.; Schlegel, H. B.; Raghavachari, K.; DeFrees, D. J.; Binkley, J. F.; Frisch, M. J.; Whitesides, R. F.; Hout, R. F.; Hehre, W. J. *Int. J. Quantum Chem. Symp.* **1981**, *15*, 269.; DeFrees, D. J.; McLean, A. D. *J. Chem. Phys.* **1985**, *82*, 333.
- Rodgers, M. T.; Armentrout, P. B. *J. Phys. Chem. A* **1997**, *101*, 2614.
- Rodgers, M. T.; Ervin, K. M.; Armentrout, P. B. *J. Chem. Phys.* **1997**, *106*, 4499.
- Chesnavich, W. J.; Bowers, M. T. *J. Phys. Chem.* **1979**, *83*, 900.
- See, for example: Sunderlin, L. S.; Armentrout, P. B. *Int. J. Mass Spectrom. Ion Processes* **1989**, *94*, 149.
- More, M. B.; Glendening, E. D.; Ray, D.; Feller, D.; Armentrout, P. B. *J. Phys. Chem.* **1996**, *100*, 1605. Ray, D.; Feller, D.; More, M. B.; Glendening, E. D.; Armentrout, P. B. *J. Phys. Chem.* **1996**, *100*, 16116. More, M. B.; Ray, D.; Armentrout, P. B. *J. Phys. Chem. A* **1997**, *101*, 831.
- Rodgers, M. T.; Armentrout, P. B. *J. Phys. Chem. A* **1997**, *101*, 1238.
- See for example, Figure 1 in ref 28.
- Armentrout, P. B.; Simons, J. *J. Am. Chem. Soc.* **1992**, *114*, 8627.
- Frisch, M. J.; Trucks, G. W.; Schlegel, H. B.; Scuseria, G. E.; Robb, M. A.; Cheeseman, J. R.; Zakrzewski, V. G.; Montgomery, J. A., Jr.; Stratmann, R. E.; Burant, J. C.; Dapprich, S.; Millam, J. M.; Daniels, A. D.; Kudin, K. N.; Strain, M. C.; Farkas, O.; Tomasi, J.; Barone, V.; Cossi, M.; Cammi, R.; Mennucci, B.; Pomelli, C.; Adamo, C.; Clifford, S.; Ochterski, J.; Petersson, G. A.; Ayala, P. Y.; Cui, Q.; Morokuma, K.; Malick, D. K.; Rabuck, A. D.; Raghavachari, K.; Foresman, J. B.; Cioslowski, J.; Ortiz, J. V.; Stefanov, B. B.; Liu, G.; Liashenko, A.; Piskorz, P.; Komaromi, I.; Gomperts, R.; Martin, R. L.; Fox, D. J.; Keith, T.; Al-Laham, M. A.; Peng, C. Y.; Nanayakkara, A.; Gonzalez, C.; Challacombe, M.; Gill, P. M. W.; Johnson, B.; Chen, W.; Wong, M. W.; Andres, J. L.; Gonzalez, C.; Head-Gordon, M.; Replogle, E. S.; Pople, J. A.; *Gaussian 98*, Revision A.3; Gaussian, Inc.: Pittsburgh, PA, 1998.
- Exploring Chemistry with Electronic Structure Methods*, 2nd ed.; Foresman, J. B., Frisch, A.; Gaussian, Inc.: Pittsburgh, PA, 1996.
- Boys, S. F.; Bernardi, R. *Mol. Phys.* **1970**, *19*, 553.
- Van Duijneveldt, F. B.; van Duijneveldt-van de Rijdt, J. G. C. M.; van Lenthe, J. H. *Chem. Rev.* **1994**, *94*, 1873.
- Hill, S. E.; Glendening, E. D.; Feller, D. *J. Phys. Chem. A* **1997**, *101*, 6125. Hill, S. E.; Feller, D.; Glendening, E. D. *J. Phys. Chem. A* **1998**, *102*, 3813.
- Nicholas, J. B.; Hay, B. P.; Dixon, D. A. *J. Phys. Chem.* **1999**, *103*, 1394.
- Becke, A. D. *J. Chem. Phys.* **1993**, *98*, 5648.
- Lee, C.; Yang, W.; Parr, R. G. *Phys. Rev. B* **1988**, *37*, 785.
- Perdew, J. P. *Phys. Rev. B* **1986**, *33*, 8822.
- Meyer, F.; Khan, F. A.; Armentrout, P. B. *J. Am. Chem. Soc.* **1995**, *117*, 9740.
- Lifshitz, C. *Adv. Mass Spectrom.* **1989**, *11*, 113.
- Møller, C.; Plesset, M. S. *Phys. Rev.* **1934**, *46*, 618.
- Bartlett, R. J. *Annu. Rev. Phys. Chem.* **1981**, *32*, 359.
- Hehre, W. J.; Radom, L.; Schleyer, P. v. R.; Pople, J. A. *Ab initio Molecular Orbital Theory*; Wiley: New York, 1986.
- Remko, M.; Sarisky, M. *Chem. Phys. Lett.* **1998**, *282*, 227.
- References 56 and 58 report G2 energies at 298 K (listed in hartrees) that agree with our G2 calculations within 18 μ h (0.05 kJ/mol). However, the 298 K enthalpies cited in ref 56 (listed in kcal/mol) are all higher by RT (which appears to be an unspecified correction for the thermal energy of the complex) compared to values derived by combining the 0 K bond enthalpies listed in Table 3 with the thermal corrections listed in Table 4. This conclusion corrects our hypothesis in ref 7 that the differences in 298 K bond enthalpies involved an incorrect conversion factor.
- Remko, M. *Chem. Phys. Lett.* **1997**, *270*, 369.
- Rothe, E. W.; Bernstein, R. B. *J. Chem. Phys.* **1959**, *31*, 1619.
- Langhoff, S. R.; Bauschlicher, C. W., Jr.; Partridge, H.; Sodupe, M. *J. Phys. Chem.* **1991**, *95*, 10677.